

Picosecond Surface Electron Dynamics on Photoexcited Si(111)(2×1) Surfaces

J. Bokor and R. Storz

AT&T Bell Laboratories, Holmdel, New Jersey 07733

and

R. R. Freeman and P. H. Bucksbaum

AT&T Bell Laboratories, Murray Hill, New Jersey 07974

(Received 21 May 1986)

Surface electrons were selectively photoexcited into the normally unoccupied antibonding surface state on the cleaved Si(111)(2×1) surface by 2.8- μm infrared laser radiation. The time decay of the antibonding-state population was then followed in real time by picosecond time-resolved uv photoemission spectroscopy. The relaxation dynamics was found to be cleavage dependent, and appears to be controlled by defects, which give rise to a unique signature in the photoemission spectra.

PACS numbers: 73.20.Cw, 79.60.Eq

Silicon crystals, on cleavage in ultrahigh vacuum to expose the (111) face, exhibit a (2×1) surface reconstruction. This surface reconstruction is of particular interest since it is metastable, i.e., following thermal annealing, the thermodynamically favored (7×7) reconstruction is produced. A wide variety of experiments aimed at elucidating the surface crystallography and electronic structure of the (2×1) surface support the π -bonded chain model originally proposed by Pandey.¹ The electronic structure of the chains exhibits an occupied surface state of bonding character denoted as π and an unfilled state of antibonding character denoted as π^* . These states are known both theoretically² and experimentally³ to be highly dispersive parallel to the chains, and nondispersive perpendicular to the chains. Optical absorption⁴ and reflectivity⁵ measurements, as well as recent photoemission measurements on highly doped *n*-type samples,⁶ give a value for the energy gap between the π and π^* states as 0.45 eV. The π^* state lies in the middle of the bulk band gap and is responsible for pinning of the Fermi level 0.40 eV above the bulk valence-band maximum at the surface of *n*-type samples.^{6,7}

We have performed the first direct measurement of the lifetime of electrons photoexcited into the π^* surface state. By use of the newly developed technique of picosecond time- and angle-resolved photoemission spectroscopy,^{8,9} population in the π^* state was followed as a function of time following excitation by a short laser pulse. The decay rates were found to be cleavage dependent, strongly implicating the role of steps and/or defects in the relaxation dynamics.

The basic principles of the measurement technique are described in detail elsewhere.⁹ Briefly, vacuum-ultraviolet radiation at 10.5-eV photon energy (118.2-nm wavelength) was produced in 80-psec-duration pulses at 10 pulses per second via ninth-harmonic conversion of the output of an amplified, mode-locked

neodymium-doped yttrium aluminum garnet (Nd:YAlG) laser operating at a wavelength of 1.06 μm . This radiation will be referred to as the probe beam, and it served as the monochromatic photon source for the photoemission measurements. The surface was photoexcited by infrared radiation at 0.44-eV photon energy (2.8- μm wavelength), produced in synchronized 80-psec-duration pulses via stimulated second Stokes Raman scattering of the Nd:YAlG laser radiation in high-pressure methane gas. This radiation will be referred to as the pump beam. Angle-resolved photoemission spectra were recorded in an ultrahigh-vacuum chamber at a pressure of $< 5 \times 10^{-11}$ Torr by a time-of-flight photoelectron spectrometer. The energy resolution of the electron spectrometer has been previously measured to be 0.1 eV at 6-eV electron energy.^{8,9} By the recording of photoemission spectra as a function of the relative arrival time of the pump and probe pulses at the sample, the decay kinetics of surface excitations can be directly observed.

Phosphorus-doped Si (111) bars ($\rho \sim 8 \Omega\text{-cm}$, $N_D \sim 3 \times 10^{14} \text{ cm}^{-3}$), of $3 \times 3 \text{ mm}^2$ cross section, were cleaved along the [2 $\bar{1}\bar{1}$] direction. Low-energy electron-diffraction (LEED) analysis was used to select cleaves which showed single-domain (2×1) reconstruction. The photoemission spectra also were used to confirm the domain structure of the surface.³

Figure 1 shows typical results obtained on high-quality cleaves. Several such cleaves gave reproducible results for photoemission spectra and relaxation dynamics. All showed sharp, high-contrast, single-domain (2×1) LEED patterns. The spectra shown in Fig. 1 were taken at an emission angle of 45° in the (0 $\bar{1}\bar{1}$) direction, corresponding to the \bar{J} point in the surface Brillouin zone (SBZ). In Fig. 1(a), a photoemission spectrum for the unexcited surface is shown. This spectrum agrees well with that obtained by Uhrberg *et al.*³ In Fig. 1(b), we show the spectrum

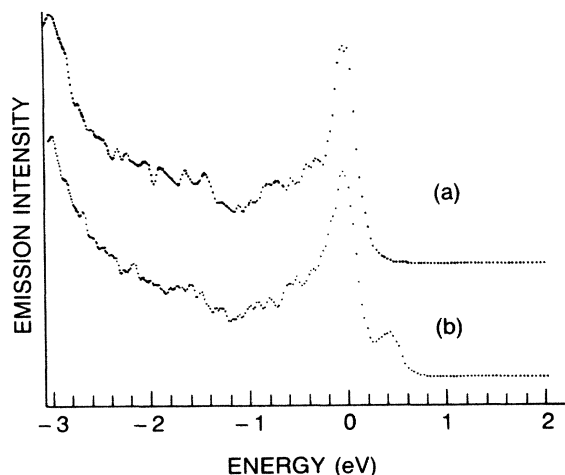


FIG. 1. Photoemission spectra from Si(111)(2 \times 1) surface at 10.5-eV photon energy. Emission angle is 45° in the (0 $\bar{1}$ 1) direction. These spectra were taken from high-quality cleaves. The energy scale has been adjusted such that zero corresponds to the position of the normally occupied π state in both spectra. (a) Conventional spectrum from unexcited surface. (b) Spectrum taken with simultaneous infrared excitation.

obtained from the photoexcited surface at exact time coincidence of the pump and probe pulses. It is remarkably similar to the photoemission spectrum of highly doped n -type silicon recently published by Mårtensson, Cricenti, and Hansson.⁶ The additional peak at 0.5 eV arises from transient population in the π^* surface state. Its emission angle is also the same as that shown in Ref. 6. The π^* population in the experiment of Mårtensson, Cricenti, and Hansson⁶ is produced by doping, and so the excess electron density can be reliably estimated as 0.01 electrons per surface atom. Since the intensity of the π^* peak in our spectra is approximately equal to that shown in Ref. 6, we deduce that the photoexcitation population is also approximately 0.01 electrons per surface atom.

The relaxation dynamics for the excited surface was studied by measurement of the signal intensity in the 0.5-eV π^* peak as a function of the relative time delay between the infrared excitation pulse and the ultraviolet probe pulse. In Fig. 2, the time-decay curve obtained from the same cleave used to obtain Fig. 1 is shown. Initially, the π^* signal rises rapidly with the excitation laser pulse, and begins to decay rapidly, essentially following the fall of the laser pulse. However, the rapid decay appears to cease, and the signal then decays much more slowly.

Figure 3 shows the results of our performing the same experiment on a cleave of "lesser" quality. The LEED pattern for this cleave was single domain, but the sharpness of the spots was slightly degraded compared to the LEED pattern taken from the cleave used

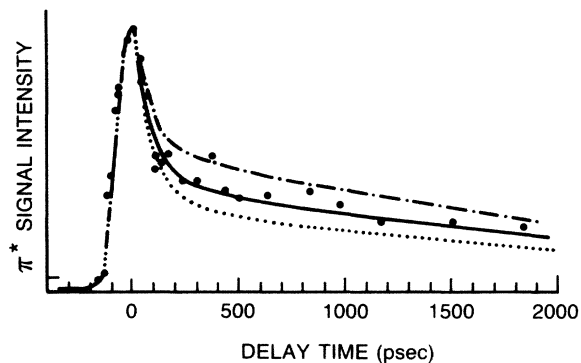


FIG. 2. Time dependence of the π^* (0.5-eV peak) signal intensity from the same cleave used to obtain Fig. 1. The experimental data are shown as bold dots. The results of the model calculation for three values of τ_h are also shown. The values of the parameters B_r and τ_e were fixed at 0.004 cm²/sec and 2.5 nsec, respectively. Solid curve, $\tau_h = 300$ psec; dotted curve, $\tau_h = 400$ psec; dot-dashed curve, $\tau_h = 200$ psec.

to obtain Fig. 1. Note that the conventional photoemission spectrum for this cleave shown in Fig. 3(a) is essentially identical to that in Fig. 1(a). The photoemission spectrum taken from the photoexcited surface of this cleave is shown in Fig. 3(b) and is clearly different from the spectrum shown in Fig. 1(b). Additional signal intensity appears in the surface band gap, and the spectrum is broadened. Optical spectroscopy,¹⁰ electron energy-loss spectroscopy,¹¹ and scanning tunneling microscopy¹² have all revealed the existence of electronic states lying within the surface band gap associated with both steps and point defects. On the basis of this and our LEED results from this cleave, we believe that this cleave has a relatively high

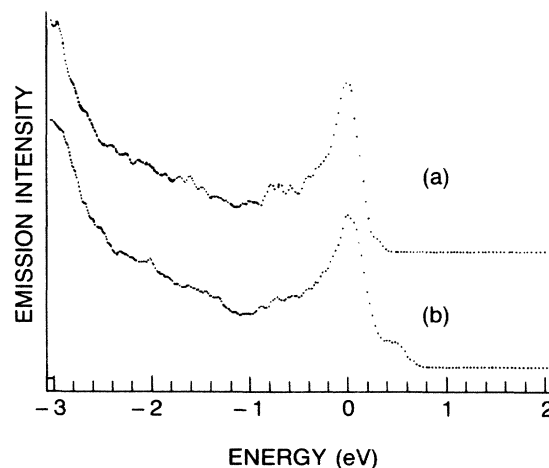


FIG. 3. Photoemission spectra obtained from a "defected" cleave under conditions identical to those used to obtain Fig. 1. (a) Unexcited surface. (b) Simultaneous infrared excitation.

density of defects as compared to the cleaves typified by photoemission spectra shown in Fig. 1. The decay curve for this cleave is shown in Fig. 4 and is clearly different from the decay curve shown in Fig. 2. These data strongly suggest that cleavage defects play a major role in the relaxation dynamics of the electronic excitations of the π -bonded chains.

It is possible to construct a model to account for the decay of the π^* population which reproduces the data obtained in the experiment. Consider the behavior of both the surface electrons excited into the π^* state and the "surface holes" which simultaneously appear in the normally occupied π state. (We have observed the surface holes directly by looking for a decrease in the π -state peak coincident in time with the maximum in the π^* -state peak. A decrease of several percent is indeed observed with a signal-to-noise ratio of about 2.) The model employs two distinct decay mechanisms to account for the two-component decay curves which are observed. The first is two-body radiative recombination of the surface electrons and holes. At the high excitation densities that are produced, this is the mechanism which leads to the fast decay. We then assume that there are different rates for the electrons and holes to scatter out of the π^* and π states. Presumably, the electrons scatter into defect or step states. The holes may also scatter into such states, or alternatively, since the energy position of the top of the normally occupied π -state band lies somewhat below the top of the bulk valence band, the surface holes may also scatter into bulk valence-band states. The abrupt end to the fast decay of the electron population is then explained by the escape of surface holes out of the π state, reducing the rate of radiative recombination.

The surface electron and hole populations thus

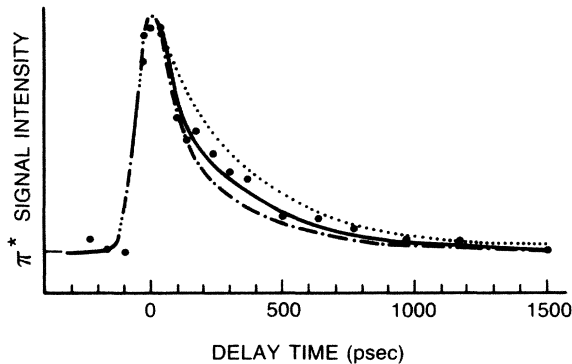


FIG. 4. Time dependence of the π^* signal intensity from the same cleave used to obtain Fig. 2. The experimental data are shown as bold dots. The results of the model calculation for three values of τ_h are also shown. The values of the parameters B_r and τ_e were fixed at 0.004 cm²/sec and 333 psec, respectively. Solid curve, $\tau_h = 100$ psec; dotted curve, $\tau_h = 50$ psec; dot-dashed curve, $\tau_h = 150$ psec.

evolve according to the following coupled differential equations:

$$dn/dt = G - B_r np - n/\tau_e, \quad (1a)$$

$$dp/dt = G - B_r np - p/\tau_h, \quad (1b)$$

where n is the density of surface electrons, p the density of surface holes, G the photoexcitation rate of surface electrons and holes, B_r the radiative recombination coefficient, τ_e the surface electron lifetime, and τ_h the surface hole lifetime. The solutions of these equations for several values of the parameters are shown as solid curves in Figs. 2 and 4.

The form of the calculated decay curves was found to be quite insensitive to the value of the radiative recombination parameter, B_r . A lower bound of 0.002 cm²/sec can be placed on B_r , below which the rapid initial decay becomes too slow to reproduce the data. However, the shape of the curve remains unchanged as B_r is increased. There is a weak dependence of the peak value of electron density on B_r . An upper bound on B_r of approximately 1.0 cm²/sec may be inferred, since at this value the calculated peak surface-electron density drops to 1×10^{12} cm⁻². For $B_r = 0.004$ cm²/sec, which is the value used for the calculated curves in Figs. 2 and 4, the peak electron density is 4×10^{12} cm⁻².

We may obtain an independent estimate of the radiative recombination coefficient B_r from the measured absorption spectrum⁴ for the π - π^* transition using the van Roosbroeck and Shockley detailed-balance method.¹³ The thermal generation rate is written as

$$R = \int_0^\infty \sigma(E) F(E) dE. \quad (2)$$

where $\sigma(E)$ is the absorption cross section, and $F(E)$ is a thermal blackbody spectrum. We obtain $R = 4.4 \times 10^{13}$ cm⁻² sec⁻¹. Then $B_r = R/n_i^2$. In order to obtain a value for n_i we must estimate the density of states near the band edges for the π and π^* surface-state bands. We used the photoemission data of Mårtensson, Cricenti, and Hansson⁶ to estimate $n_i^2 = (3 \pm 2) \times 10^{16}$ cm⁻⁴. We therefore obtain $B_r = (2.7 \pm 1.8) \times 10^{-3}$ cm²/sec, which is in good accord with the results of our model fit to the data.

The best fit to the data in Fig. 2 gives $\tau_e = 2.5 \pm 0.3$ nsec and $\tau_h = 300 \pm 100$ psec. The best fit to the data in Fig. 4 gives $\tau_e = 330 \pm 30$ psec and $\tau_h = 100 \pm 50$ psec. (Within the quoted error bars, the optimum values for these parameters were not sensitive to the value of B_r used in the calculation.) Thus we see that on the defected cleave, both the electron and hole lifetimes decrease. This tends to suggest that the hole lifetime, τ_h , is dominated by scattering of holes out of the π state and into defect states. However, since the bulk valence-band maximum lies at $\bar{\Gamma}$, the center of the SBZ, and the maximum of the π surface-state

band lies at \bar{J} , the edge of the SBZ, it is possible that steps and defects could also increase the rate for hole scattering from the π state to the bulk valence band.

In summary, we have performed the first direct measurement of the decay dynamics of electrons photoexcited into the π^* antibonding surface state and holes photoexcited into the π bonding surface state on the cleaved Si(111) (2×1) surface. The dynamics is found to be cleavage dependent, strongly suggesting that steps and defects are playing an important role in the dynamics. An estimate for the surface radiative recombination coefficient was obtained from the experiment which is in agreement with that calculated from the experimentally measured absorption coefficient.

¹K. C. Pandey, Phys. Rev. Lett. **47**, 1913 (1981).

²J. E. Northrup and M. L. Cohen, Phys. Rev. Lett. **49**, 1349 (1982).

³R. I. G. Uhrberg, G. V. Hansson, J. M. Nicholls, and

S. A. Flodström, Phys. Rev. Lett. **48**, 1032 (1982).

⁴M. A. Olmstead and N. M. Amer, Phys. Rev. Lett. **52**, 1148 (1984).

⁵P. Chiaradia, A. Cricenti, S. Selci, and G. Chiarotti, Phys. Rev. Lett. **52**, 1145 (1984).

⁶P. Mårtensson, A. Cricenti, and G. V. Hansson, Phys. Rev. B **32**, 6959 (1985).

⁷F. J. Himpsel, G. Hollinger, and R. A. Pollack, Phys. B **28**, 7014 (1983).

⁸R. Haight, J. Bokor, J. Stark, R. H. Storz, R. R. Freeman, and P. H. Bucksbaum, Phys. Rev. Lett. **54**, 1302 (1985).

⁹J. Bokor, R. Haight, J. Stark, R. H. Storz, R. R. Freeman, and P. H. Bucksbaum, Phys. Rev. B **32**, 3669 (1985).

¹⁰P. Chiaradia, G. Chiarotti, S. Selci, and Z. Zhi-Ji, Surf. Sci. **132**, 62 (1983).

¹¹N. J. DiNardo, J. E. Demuth, W. A. Thompson, and Ph. Avouris, Phys. Rev. B **31**, 4077 (1985).

¹²R. M. Feenstra, W. A. Thompson, and A. P. Fein, Phys. Rev. Lett. **56**, 608 (1986); R. M. Feenstra and J. Stroscio, unpublished.

¹³J. I. Pankove, *Optical Processes in Semiconductors* (Dover, New York, 1971).